

# Heart Position Uncertainty Quantification in the Inverse Problem of ECGI

Jake A Bergquist<sup>1,2,3</sup>, Lindsay C Rupp<sup>1,2,3</sup>, Anna Busatto<sup>1,2,3</sup>, Ben Orkild<sup>1,2,3</sup>, Brian Zenger<sup>4</sup>, Wilson Good<sup>5</sup>, Jaume Coll-Font<sup>5</sup>, Akil Narayan<sup>1,7</sup>, Jess Tate<sup>1</sup>, Dana Brooks<sup>6</sup>, Rob S MacLeod<sup>1,2,3</sup>

<sup>1</sup> Scientific Computing and Imaging Institute, University of Utah, SLC, UT, USA

<sup>2</sup> Nora Eccles Treadwell CVRTI, University of Utah, SLC, UT, USA

<sup>3</sup> Department of Biomedical Engineering, University of Utah, SLC, UT, USA

<sup>4</sup> School of Medicine, University of Utah, SLC, UT, USA

<sup>5</sup> Acutus Medical, Carlsbad, CA, USA

<sup>6</sup> Department of Electrical and Computer Engineering, Northeastern University, Boston, MA, USA

<sup>7</sup> Department of Mathematics, University of Utah, SLC, UT, USA

## Abstract

*Electrocardiographic imaging (ECGI) is a clinical and research tool for noninvasive diagnosis of cardiac electrical dysfunction. The position of the heart within the torso is both an input and common source of error in ECGI. Many studies have sought to improve cardiac localization accuracy, however, few have examined quantitatively the effects of uncertainty in the position of the heart within the torso. Recently developed uncertainty quantification (UQ) tools enable the robust application of UQ to ECGI reconstructions. In this study, we developed an ECGI formulation, which for the first time, directly incorporated uncertainty in the heart position. The result is an ECGI solution that is robust to variation in heart position. Using data from two Langendorff experimental preparations, each with 120 heartbeats distributed across three activation sequences, we found that as heart position uncertainty increased above  $\pm 10$  mm, the solution quality of the ECGI degraded. However, even at large heart position uncertainty ( $\pm 40$  mm) our novel UQ-ECGI formulation produced reasonable solutions (root mean squared error  $< 1$  mV, spatial correlation  $> 0.6$ , temporal correlation  $> 0.75$ ).*

## 1. Introduction

Electrocardiographic imaging (ECGI) is an established technique for reconstructing cardiac bioelectric activity from noninvasive measurements of body-surface potentials. It is used in both research and clinic, with several commercial implementations on the market.[1] ECGI implementations rely on many subject-specific measurements and the position of the heart within the torso is both one of these inputs and a common source of error. Many stud-

ies have aimed to minimize this cardiac localization error.[2,3] However, few studies have investigated quantitatively how uncertainty in the heart position affects the resulting ECGI solution[4, 5] and none to our knowledge have attempted to account for this uncertainty in the ECGI formulation. Neglecting to account for heart position uncertainty could limit the clinical utility of ECGI.

Uncertainty quantification (UQ) provides a mathematically robust and efficient means to study model response to inevitable, often only approximately known, variability in model inputs. Recent progress in both the theory and implementations of UQ has supported its application to ECGI.[4, 6] However, a challenge in applying UQ to ECGI is that most applications of UQ have been to forward problems, [5, 7] whereas ECGI is an inverse problem.[1] A forward problem implements a generally well-behaved relationship between input parameters and a response that is uniquely defined. Inverse problems may use the same underlying model but seek to identify the inputs using measured outputs, a problem that is often ill-posed and whose solution may not be unique. Consequently, UQ is not commonly applied to inverse problems such as ECGI.[4] However, developing inverse formulations that account for, and are robust to, variability in the input parameters is critical for producing reliable and useful clinical and research implementations of ECGI.

Here, we developed a new formulation of ECGI that expands the standard assumption of a single fixed cardiac geometry to an assumption of a distribution of possible cardiac position dictated by uncertainty in the position. This research represents a first attempt to directly include the uncertainty of heart position in an ECGI formulation. Our approach is based on our previous ECGI formulation,[2, 8] which we named the “joint-inverse” solution. We leveraged this joint-inverse approach and recently developed

UQ tools to produce a robust application of UQ to the ECGI inverse problem.

## 2. Methods

**Uncertainty Quantification:** Traditional parametric UQ approaches identify statistical moments such as the mean, standard deviation, and sensitivity of model output given a probabilistic characterization of variability in some of its inputs.[6] In this study, rather than calculating statistical moments, we designed an ECGI inverse formulation that can incorporate variability in an input parameter. The first step in this process was to generate samples of the variable input parameter, which we achieved by applying weighted approximate Fekete sampling (WAFS).[6] WAFS produces weighted samples given a set of parameters and their associated distributions. In this study we described heart position as the  $3 \times 1$  parameter vector  $\vec{p}$  whose elements were the X, Y, Z components of a translation applied to the cardiac geometry from its nominal position. The WAFS parameter samples ( $\vec{p}_1 \dots \vec{p}_N$ ) and associated weights ( $w_1 \dots w_N$ ) were drawn from a beta distribution with  $\alpha = 2, \beta = 2$ . The samples were selected to satisfy a  $5^{th}$  degree polynomial chaos expansion fit. The open-source UQ software framework UncertainSCI was used to obtain the samples and weights.[6]

**ECGI Formulation:** We incorporated the WAFS sampled cardiac positions into a single ECGI solution using our joint-inverse formulation[8], which combines multiple instances of the inverse problem into a single equation that solves for a single cardiac source. In this case the multiple inverse problem instances come from the cardiac position samples.

We modeled the bioelectric sources ( $\Phi_H$ ) as extracellular potentials defined on a pericardiac surface. A boundary element method was used to generate the transfer matrix ( $\mathbf{A}$ ), which defined the forward projection to the body-surface potentials ( $\Phi_T$ ).[9] The matrix  $\mathbf{A}$  captures the geometry of the torso and so is a function of the heart position parameters  $\vec{p}$ . To combine the multiple heart positions from WAFS as variations in the forward model we created the block matrices  $\hat{\Phi}_T$  and  $\hat{\mathbf{A}}$  as

$$\hat{\Phi}_T = \begin{bmatrix} \Phi_T \cdot w_1 \\ \Phi_T \cdot w_2 \\ \Phi_T \cdot w_3 \\ \dots \\ \Phi_T \cdot w_N \end{bmatrix}, \hat{\mathbf{A}} = \begin{bmatrix} \mathbf{A}(\vec{p}_1) \cdot w_1 \\ \mathbf{A}(\vec{p}_2) \cdot w_2 \\ \mathbf{A}(\vec{p}_3) \cdot w_3 \\ \dots \\ \mathbf{A}(\vec{p}_N) \cdot w_N \end{bmatrix}, \quad (1)$$

where the BSP matrix in  $\hat{\Phi}_T$  is a copy of  $\Phi_T$  weighted by  $w_1$  through  $w_N$ . Each forward matrix in  $\hat{\mathbf{A}}$  is a function of the heart position  $\mathbf{A}(\vec{p}_i)$  for ( $\vec{p}_1 \dots \vec{p}_N$ ) weighted by  $w_1 \dots w_N$ . These matrices are then combined into a modified Tikhonov inverse equation,

$$\operatorname{argmin}_{\Phi_H} \|\hat{\mathbf{A}} \Phi_H - \hat{\Phi}_T\|_F^2 + \lambda \|\mathbf{R} \Phi_H\|_F^2, \quad (2)$$

where we selected the regularization matrix  $\mathbf{R}$  as the surface Laplacian operator (Tikhonov  $2^{nd}$  order), and set the regularization weight  $\lambda$  according to the Frobenius L-curve criterion.[2] The resulting solution to the inverse formulation in Eq 2 represents an expected value of the inverse problem over the variation in cardiac position, and we refer to this as the UQ joint-inverse solution.

**Data Sets:** We recorded cardiac potentials from a modified Langendorff preparation described previously.[10] Briefly, an explanted, perfused canine heart was suspended in a torso-shaped electrolytic tank embedded with 192 electrodes. We instrumented the heart with a 256-electrode pericardiac cage. Potentials from both the torso tank and cage electrodes were recorded simultaneously at 1000 sample/s. We recorded three activation sequences: sinus rhythm, and pacing at 171 bpm from ventricular needles placed in the anterior (aVP) and posterior (pVP) left ventricle. We captured 40 heartbeats for each activation sequence (sinus, aVP, pVP). Signals were filtered, baseline corrected, and fiducialized using PFEIFER[11], and geometries were acquired as described previously.[10] We replicated this experimental procedure twice, producing two data sets (Data Set 1 and Data Set 2). All experiments were approved by the Institutional Animal Care and Use Committee of the University of Utah, protocol number 17-04016 approved on 05/17/2017. We used the registered position of the pericardiac cage as the nominal heart position, which we numerically translated to match the sampled positions as described above. To examine the effect of increasing position uncertainty, we selected 8 different ranges for the beta distributions of heart translations (Ranges 1 through 8:  $\pm 1$  mm,  $\pm 5$  mm,  $\pm 10$  mm,  $\pm 15$  mm,  $\pm 20$  mm,  $\pm 25$  mm,  $\pm 30$  mm,  $\pm 40$  mm).

**Inverse Solution Evaluation:** We first computed an inverse solution for each heartbeat using the nominal heart position. We then calculated the UQ joint-inverse solution using the WAFS samples and weights from the 8 ranges. Thus, we produced 9 sets of inverse solutions for each beat of each activation sequence in each dataset (1 nominal, 8 UQ). We compared these inverse solutions to the measured pericardiac potentials in terms of the root mean squared error (RMSE), temporal correlation (TC), and spatial correlation (SC).[10] Furthermore, we examined the performance of the inverse estimates in terms of the regularization weight  $\lambda$  chosen by our L-curve procedure for each inverse solution and the curvature of the L-curve corner ( $\kappa$ ) defined as the maximum second derivative of a cubic spline interpolation of the L-curve.

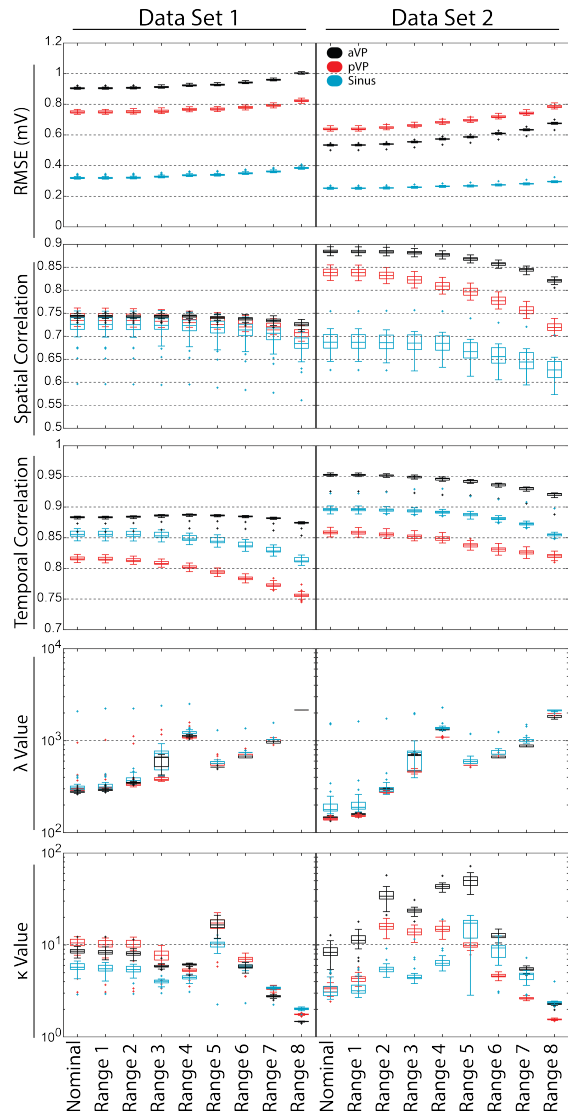


Figure 1. ECGI accuracy and inverse problem metrics. Each row shows a metric, top to bottom: RMSE (mV), Spatial Correlation, Temporal Correlation,  $\lambda$  value,  $\kappa$  value. Metrics are shown in each panel as box plots for each set of inverse solutions, from left to right: nominal position, then ranges 1 through 8. The panels in the left column correspond to Data Set 1 and in the right column to Data Set 2. Each box plot represents the metric for all 40 heartbeats for a given activation sequence and data set (Black: aVP, red: pVP, cyan: sinus). Outliers (plus signs) are defined as values that are 1.5 times the interquartile range away from the bottom or top of the box. Note that the  $\lambda$  and  $\kappa$  plots are in log scale.

### 3. Results

As heart position range increased (from  $\pm 1$  mm, Range 1 to  $\pm 40$  mm, Range 8), the quality of the inverse solution degraded. We observed this degradation as increasing RMSE and decreasing SC and TC in Figure 1. Increasing range corresponded to an increase in  $\lambda$  and a decrease in  $\kappa$  value for the largest ranges. However, notably, the  $\kappa$  value increased at smaller ranges, around  $\pm 20$  mm (range 5) in Data Set 1, and around  $\pm 5$  mm to  $\pm 20$  mm (range 2 to 5)

in Data Set 2, followed by a falloff at larger ranges.

Figure 2 shows examples of inverse reconstructions from each position range as well as the nominal position of the heart. The increase in uncertainty ranges resulted most notably in changes in the shape and location of the potential depressions across the cage.

### 4. Discussion and Conclusions

In this study, we report for the first time to our knowledge ECGI solutions that incorporate uncertainty in the position of the heart by applying our joint-inverse formulation. For small position uncertainty ranges ( $\leq \pm 10$  mm), the UQ ECGI solutions were close to those found using the nominal heart position according to RMSE, SC, and TC. The major benefit of this UQ approach is that it provides confidence that uncertainty in the heart position has been accounted for in the ECGI solution. Thus, the UQ solution may be preferable even if it is similar to the nominal solution.

Another benefit of the UQ ECGI formulation is that it allows us to explore the effect of heart position variability on the ECGI inverse solution directly, rather than through inferences made about the forward problem as in previous studies.[5] With ranges above  $\pm 10$  mm, the resulting UQ ECGI solutions displayed a decrease in quality as shown by low SC, and TC. The RMSE, however, was consistently within 0.2 mV for each activation sequence across all position ranges. The larger ranges of position variability matched increasing levels of regularization, *i.e.*, an increase in  $\lambda$  value and a decrease in  $\kappa$  values, suggesting smoother L curves. Our study was limited to using the L-curve criterion, and other  $\lambda$  selection methods might be preferable. Despite this limitation, even the largest range of position uncertainty ( $\pm 40$  mm) produced ECGI solutions that appeared qualitatively reasonable (Figure 2).

The increase in L-corner sharpness (as indicated by increased  $\kappa$  values) at the middle ranges (centered around  $\pm 20$  mm for Data Set 1 and  $\pm 15$  mm for Data Set 2) supports a previous finding that the shape of the L curve may serve as an indicator of how well localized the cardiac geometry is within the torso.[3] Our findings support the hypothesis that this increase in  $\kappa$  may be related to levels of geometric uncertainty.

We and others have developed methods for correcting the heart position using augmented parameterizations of heart position;[2, 3, 12, 13] however, all have significant limitations under realistic scenarios. It is also not clear what effects lingering geometric errors have and what level of heart position accuracy is necessary. This study provides quantifiable levels of robustness for inverse solutions under assigned heart position variability. These results are a step towards understanding how lingering geometric errors affect the inverse solutions and what level of geomet-

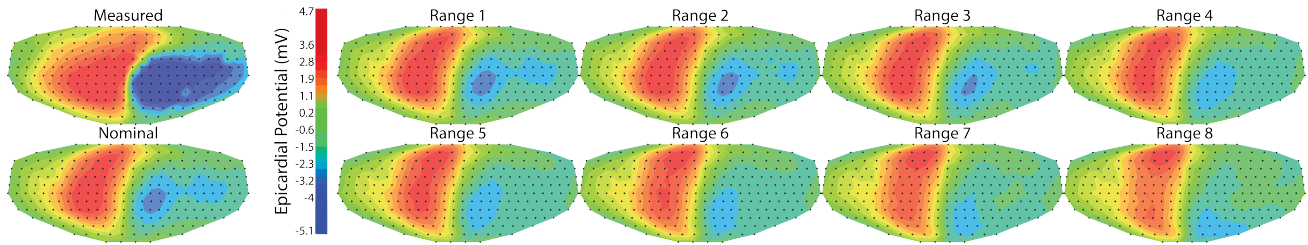


**Figure 2.** Inverse solutions as compared to the measured epicardial potentials for an example beat of the pVP activation sequence from Data Set 1. The measured pericardiac potentials (top left) and the inverse solution found using the nominal heart position (bottom left) are on the left side of the color bar. On the right of the color bar are the 8 inverse solutions calculated using each of the 8 position ranges. All potential maps (mV) are shown at the peak of the RMS of the measured pericardiac signal. Potentials are displayed on a flattened unwrapped projection of the cage geometry.

ric accuracy is necessary to produce robust solutions. Although this study was limited to translations of heart position, extensions would be straightforward for additional positional parameters *e.g.*, rotations. Future studies will examine the effects of uncertainties in conductivity values, positions of other organs, and heart shape.

## Acknowledgments

Support for this research came from the Center for Integrative Biomedical Computing ([www.sci.utah.edu/cibc](http://www.sci.utah.edu/cibc)), NIH/NIGMS grants P41 GM103545 and R24 GM136986, NIH/NIBIB grant U24EB029012, and the Nora Eccles Harrison Foundation for Cardiovascular Research.

## References

- [1] Cluitmans M, Brooks D, MacLeod R, Dossel O, Guillem M, van Dam P, Svehlikova J, He B, Sapp J, Wang L, Bear L. Validation and opportunities of electrocardiographic imaging: From technical achievements to clinical applications. *Front Physiol* 2018;9:1305.
- [2] Bergquist JA, Coll-Font J, Zenger B, Rupp LC, Good WW, Brooks DH, MacLeod RS. Noninvasive reconstruction of cardiac position using body surface potentials. *Computers in Biology and Medicine* 2022;142:105–174. ISSN 0010-4825.
- [3] Rodrigo M, Climent AM, Liberos A, Hernandez-Romero I, Arenal A, Bermejo J, Fernandez-Aviles F, Atienza F, Guillem MS. Solving inaccuracies in anatomical models for electrocardiographic inverse problem resolution by maximizing reconstruction quality. *IEEE Transactions on Medical Imaging* 2018;37(3):733–740.
- [4] Tate JD, Good WW, Zemzemi N, Boonstra M, van Dam P, Brooks DH, Narayan A, MacLeod RS. Uncertainty quantification of the effects of segmentation variability in ecgi. In Ennis DB, Perotti LE, Wang VY (eds.), *Functional Imaging and Modeling of the Heart*. Cham: Springer International Publishing. ISBN 978-3-030-78710-3, 2021; 515–522.
- [5] Swenson D, Geneser S, Stinstra J, Kirby R, MacLeod R. Cardiac position sensitivity study in the electrocardiographic forward problem using stochastic collocation and BEM. *Annal Biomed Eng* Dec. 2011;30(12):2900–2910.
- [6] Rupp LC, Liu Z, Bergquist JA, Rampersad S, White D, Tate JD, Brooks DH, Narayan A, MacLeod RS. Using uncertainty to quantify uncertainty in cardiac simulations. In 2020 *Computing in Cardiology*. 2020; 1–4.
- [7] Bergquist JA, Zenger B, Rupp LC, Narayan A, MacLeod RS. Uncertainty quantification in simulations of myocardial ischemia. In 2021 *Computing in Cardiology*, in Press. 2021; 1–4.
- [8] Bergquist JA, Coll-Font J, Zenger B, Rupp LC, Good WW, Brooks DH, MacLeod RS. Simultaneous multi-heartbeat ecgi solution with a time-varying forward model: a joint inverse formulation. In Ennis DB, Perotti LE, Wang VY (eds.), *Functional Imaging and Modeling of the Heart*. Cham: Springer International Publishing, 2021; 493–502.
- [9] Burton B, Tate J, Erem B, Swenson D, Wang D, Brooks D, van Dam P, MacLeod R. A toolkit for forward/inverse problems in electrocardiography within the SCIRun problem solving environment. In *Proceedings of the IEEE Engineering in Medicine and Biology Society 33rd Annual International Conference*. IEEE Eng. in Med. and Biol. Soc., 2011; 1–4.
- [10] Bergquist JA, Good WW, Zenger B, Tate JD, Rupp LC, MacLeod RS. The electrocardiographic forward problem: A benchmark study. *Computers in Biology and Medicine* 2021;134:104–476. ISSN 0010-4825.
- [11] Rodenhauer A, Good W, Zenger B, Tate J, Aras K, Burton B, MacLeod R. PFEIFER: Preprocessing framework for electrograms intermittently fiducialized from experimental recordings. *J Open Source Software* September 2018; 3(21):472.
- [12] Coll-Font J, Brooks DH. Tracking the position of the heart from body surface potential maps and electrograms. *Frontiers in Physiology* 2018;9:1727.
- [13] Toloubidokhti M, Gyawali PK, Gharbia OA, Jiang X, Font JC, Bergquist JA, Zenger B, Good WW, Brooks DH, MacLeod RS, Wang L. Deep adaptive electrocardiographic imaging with generative forward model for error reduction. In Ennis DB, Perotti LE, Wang VY (eds.), *Functional Imaging and Modeling of the Heart*. Cham: Springer International Publishing, 2021; 471–481.

Address for correspondence:

Jake Bergquist  
University of Utah  
72 Central Campus Dr, Salt Lake City, UT 84112  
[jbergquist@sci.utah.edu](mailto:jbergquist@sci.utah.edu)